Indium adlayer kinetics on the gallium nitride (0001) surface: Monitoring indium segregation and precursor-mediated adsorption

Soojeong Choi,[1] Tong-Ho Kim,[2] Scott Wolter,[2] April Brown,[2] Henry O. Everitt,[1,2] Maria Losurdo,[3] and Giovanni Bruno[3]
[1]*Department of Physics, Duke University, Durham, North Carolina 27708, USA*
[2]*Department of Electrical and Computer Engineering, Duke University, Durham, North Carolina 27708, USA*
[3]*Institute of Inorganic Methodologies and of Plasmas-CNR, via Orabona, 4-70126 Bari, Italy*
(Received 7 August 2007; revised manuscript received 22 October 2007; published 20 March 2008)

Indium kinetics and evidence for indium segregation on the GaN (0001) surface are investigated via *in situ* spectroscopic ellipsometry. Indium deposition exhibits two stable states at coverages of 1.0 and 1.7 ML within the temperature range of 630–688 °C. Formation of each layer is governed by two kinetic processes: nuclei formation and nuclei-mediated layer adsorption. The measured desorption activation energies of nuclei of the first (2.04 eV) and second (2.33 eV) monolayers are lower than the desorption activation energies of the aggregated first (2.64 eV) and second (2.53 eV) monolayers, respectively. This suggests that adatoms preferentially interact with the nuclei and laterally aggregate.

DOI: 10.1103/PhysRevB.77.115435 PACS number(s): 81.15.Hi, 78.20.Ci, 81.70.Fy

I. INTRODUCTION

It is now broadly accepted that during III-N semiconductor growth using molecular beam epitaxy (MBE), a metallic adlayer forms that increases the diffusion length of adatoms and induces a smooth surface morphology.[1,2] Indium, which is an important constituent of the III-N semiconductor system, possesses the largest atomic size and weight of all the group III metallic components. As compared to gallium on GaN surfaces, there have only been a few studies of the kinetics of indium wetting and growth on III-N surfaces.[2–4] However, it has been empirically observed that indium acts as a surfactant for III-N material growth and segregates during InGaN quantum well growth. As a surfactant, indium can increase the surface III/V ratio, making it easier to achieve metal-rich conditions during the growth of other III-N semiconductors, without incorporating indium into the bulk or forming droplets of other materials.[4–6] Conversely, several research groups have reported that indium is incorporated nonuniformly in InGaN films and quantum wells, resulting in dispersion of the band edge.[7–9] These two characteristics of indium imply that the interaction between adatoms is stronger than the interaction between adatoms and dangling bonds terminating the surface.

II. EXPERIMENTAL DETAIL

To understand this more fully, the indium adsorption-desorption kinetics on GaN (0001) is investigated *in situ* by monitoring the variation of the imaginary part of the pseudodielectric function measured with spectroscopic ellipsometry (SE). SE has unique advantages over other *in situ* monitoring techniques since it is an optical, real-time, nonintrusive, and nonperturbing technique that directly monitors surfaces with monolayer (ML) sensitivity. As such, it measures the temporal evolution of adlayer coverage as overlayers are formed. In particular, for a thin absorbent metallic adlayer, the imaginary part of pseudodielectric function varies proportionally to the adlayer thickness.[10]

Here, we report the use of *in situ* SE to monitor indium adlayers deposited on a GaN (0001) surface in order to understand how the growth kinetics depend on temperature, deposition rate, and deposition time. Studies were performed in a VEECO Gen II MBE system installed with SE (UVISEL, Horiba Jobin Yvon) operating in the photon energy range of 1.5–6.5 eV. A hydride vapor phase epitaxy grown GaN (0001) template was used as substrate, whose surface was prepared by degassing, followed by a Ga flash-off deoxidation process, as reported in our previous work.[11] Indium adsorption-desorption is investigated for indium beam equivalent pressures (BEPs) in the range of 4.96×10^{-9}–7.59×10^{-7} Torr and for substrate temperatures in the range of 630–688 °C, with a temperature uncertainty of ±15 °C.

III. GROWTH KINETICS

As previously reported for Ga on GaN,[11] the imaginary part of the pseudodielectric function ($\langle\varepsilon_2\rangle$) of In on a GaN surface was observed to monotonically and linearly vary with In adlayer coverage for the first two monolayers. Figure 1(a) shows the evolution of the $\langle\varepsilon_2\rangle$ spectra during In nucleation on GaN for an In BEP of 2.41×10^{-7} Torr. Because this incident flux is much higher than the desorption rate at the substrate temperature of 630 °C, In adlayer coverage linearly increases with time. The $\langle\varepsilon_2\rangle$ spectra, measured each second during this deposition, also shows a monotonic linear increase over the spectral range of 2.5–5.5 eV, confirming a linear relationship between $\langle\varepsilon_2\rangle$ and adlayer coverage for the first two monolayers. Following deposition, the evolution of the spectrum during In desorption reversed [Fig. 1(b)], recovering the original spectrum once all In adatoms desorb. This implies that after a cycle of deposition and desorption, the surface is not chemically altered. Therefore, the variation of $\langle\varepsilon_2\rangle$ monitored at any photon energy in this range can be used for the analysis of In thickness. All kinetic data reported here were analyzed at 3 eV because the light source was brightest there.

Ideally, adlayer thickness is obtained by decomposing the measured $\langle\varepsilon_2\rangle$ spectrum of In/GaN into the constituent real

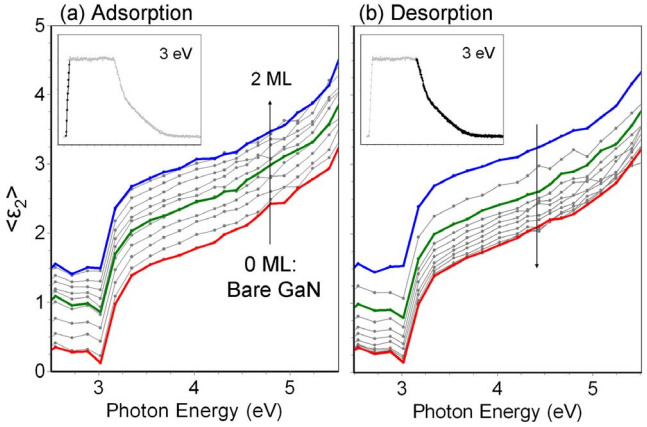

FIG. 1. (Color online) Evolution of $\langle \varepsilon_2 \rangle$ in the spectral range of 2.5–5.5 eV during (a) deposition-adsorption and (b) desorption. Each spectrum is taken every second during deposition and every 20 s during desorption. For deposition with incident flux of 2.41×10^{-7} Torr and substrate temperature of 630 °C, the adsorption rate is much higher than desorption from the adsorbed layer, so the $\langle \varepsilon_2 \rangle$ spectra linearly increase with deposition time. The highlighted thick solid spectra correspond to bare GaN (red), 1 ML In coverage (green), and 2 ML In coverage (blue). The insets show the temporal evolution of $\langle \varepsilon_2 \rangle$ at 3 eV.

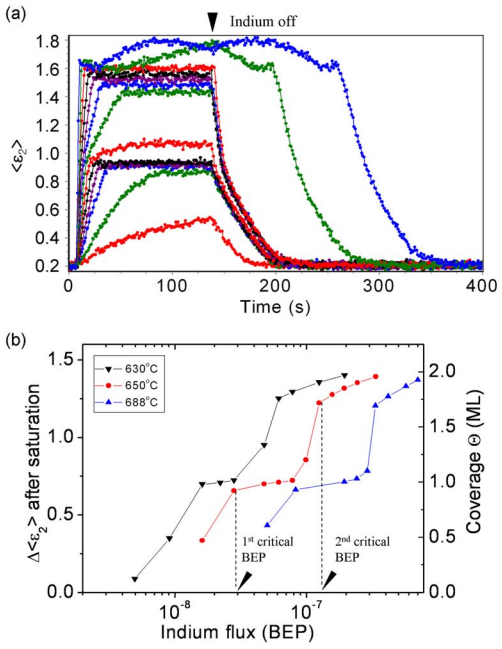

FIG. 2. (Color online) (a) Imaginary part of the pseudodielectric function $\langle \varepsilon_2 \rangle$ at 3 eV as a function of indium flux between 1.61×10^{-8} and 7.59×10^{-7} Torr, with fixed deposition time (130 s) and substrate temperature (650 °C). (b) Steady-state coverage as a function of indium flux for substrate temperatures of 630, 650, and 688 °C. In this temperature range, stable states are observed at 1 ML and 1.7 ML.

dielectric functions of In and GaN at the temperature of interest, then fitting to obtain the respective thicknesses. The actual temperature-dependent GaN dielectric function was well approximated by the GaN pseudodielectric function measured by SE before In deposition. The temperature-dependent In spectrum is unknown; so, as was done previously for Ga,[11] the composite In/GaN spectrum was measured by SE, the GaN pseudodielectric function subtracted, and the residual In spectrum was fit by a simple Drude-type dispersion curve, whose fitting parameters ε_∞ (high frequency limit=1.9), ω_p (plasma frequency, $\hbar\omega_p$=14.3 eV), and τ (relaxation time, $\hbar/\tau$=1.7 eV) were held constant over the temperature range of this experiment. As will be seen below, this simple procedure adequately and self-consistently provided reproducible analyses that agreed with the published literature, so a more complex model is not warranted by the data. As will be shown below, the thick green line spectrum in Fig. 1(a) corresponds to the first "plateau," i.e., 1 ML coverage. The above analysis returns a 1 ML In adlayer thickness of ~2.7 Å at 630 °C, which compares well with a recent report of 2.23 Å at 300 K.[12]

Figure 2(a) shows the variation of the imaginary part of the pseudodielectric function during the adsorption and desorption of indium for a series of indium BEPs with fixed deposition time (130 s) and substrate temperature (650 °C). When the indium shutter is opened, $\langle \varepsilon_2 \rangle$ starts to increase due to the formation of an indium adlayer, then a steady-state coverage is reached. At steady state, adlayer adsorption and desorption reach dynamic equilibrium so that surface coverage remains constant during continued deposition. This dynamic equilibrium reflects a constantly evolving microscopic surface morphology for a given steady-state coverage but randomly fluctuating structural manifestations (e.g., domain polarization and site-to-site percolation) of this evolution average out on the slow time scale (1 s) and large size (5 mm^2) of the measurements. Indeed, this technique is compelling and reproducible precisely because it only measures the average aggregate coverage during dynamic equilibrium, independent of microscopic fluctuations and structural idiosyncrasies.[13] Identical deposition experiments were performed for three different substrate temperatures (630, 650, and 688 °C). The steady-state coverage at each temperature, which is determined by the average of the data points after saturation, is plotted as a function of indium BEP in Fig. 2(b). The exception to this procedure is for the lowest BEP corresponding to a curve, which is not fully saturated during the 130 s deposition time. For this case, the adsorption curve is fitted by using a single exponential function, and the saturation value is extrapolated. BEPs, corresponding to the reference flux of impinging atoms, are measured by using ion gauge located in the sample position.

For a given temperature, the steady-state coverage increases as the indium flux increases, then slows dramatically at a "critical" BEP [e.g., 2.3×10^{-8} Torr for 650 °C in Fig. 2(b)]. Note that this critical BEP increases with increasing temperature, as does the range of flux values over which this slow growth is manifested. However, analysis of the pseudodielectric spectrum indicates that the adatom coverage plateau is the same $\Theta \approx 1$ ML ($\langle \varepsilon_2 \rangle \approx 0.9$) for all temperatures. Thus, the critical flux where the plateau starts corresponds to the completion of 1 ML coverage. For fluxes above this critical BEP in the plateau region, the slow growth in coverage suggests that the additional adatoms quickly desorb

off of the first monolayer before they can sufficiently nucleate the second monolayer. The plateau ends when the flux is high enough to counteract this rapid desorption and complete the nucleation of the second monolayer. Since the steady-state coverage at the end of the plateau is only slightly higher than at the beginning, the nucleation layer coverage required to commence formation of the second monolayer is much less than 1 ML.

After sufficient nuclei have formed, the plateau ends and the steady-state coverage starts to increase again with further increase of the indium flux, indicating rapid growth of the second monolayer. Eventually, the steady-state coverage suddenly slows again upon reaching 1.7 ML [$\langle\varepsilon_2\rangle=1.45$ in Fig. 2(a)], beginning another plateau at a second critical incident BEP [as shown in Fig. 2(b)]. The abrupt changes between the stable states indicate that the quasiequilibrium coverage of $\Theta<1.0$ ML and 1.0 ML$<\Theta<1.7$ ML only occur within a narrow range of deposition conditions. Above the second critical BEP, the steady-state coverage slowly increases toward $\Theta=2$ ML ($\langle\varepsilon_2\rangle=1.60$) with increasing BEP.

This may be understood as follows. For Ga-terminated surfaces in wurtzitic GaN, three of four Ga bonds connect nearest neighbor atoms, leaving one Ga dangling bond. For an indium adatom residing on this Ga-terminated surface, one orbital of indium interacts with the Ga dangling bond of the surface, the beginning of nuclei formation. The remaining three dangling bonds subsequently interact with nearest adatoms, forming a trigonal planar structure on the surface, which begins the lateral growth of the layer. Therefore, the 1 ML indium surface is in registry to the underlying Ga atoms so no surface dangling bonds remain. Additional indium adatoms forming the second monolayer have a tendency to recover the bulk indium properties as compared to the first monolayer because they are not forced into registry with the underlying Ga layer. Since the atomic size of indium is larger than gallium, ~0.7 ML of indium (expressed in units of Ga surface site density) is sufficient to cover the surface.

In Fig. 2(a), we see evidence of this emerging bulklike behavior by the indium adatoms. Notice that for the highest fluxes, the character of the curves changes in two significant ways. First, the desorption of the two-dimensional wetting layer is delayed after deposition termination by an amount proportional to the deposition times. As was seen in Ga deposition on GaN (0001),[11] this is a clear indication that the growth mode has changed from forming two-dimensional wetting layers to forming three-dimensional indium droplets on the surface. Now, the relationship between indium coverage and $\langle\varepsilon_2\rangle$ variation fails to be linear when the deposition mode changes to three-dimensional droplet formation. Droplet-induced lateral nonuniformities on a scale of the incident light wavelength induce depolarization of reflected light, altering the measured SE signal as the droplet size and spacing evolve with continued deposition. This effect is at least partially responsible for the second change in character of the curves in Fig. 2(a): the small temporal $\langle\varepsilon_2\rangle$ oscillations at the two highest fluxes. [Note that the steady-state coverage for these fluxes is not presented in Fig. 2(b).] Thus, we conclude that after indium atoms cover 2 ML on the GaN (0001) surface, excess indium atoms start to form nucleation sites on the wetting layer and ripen into droplets.

During the delay between deposition termination ["indium off" in Fig. 2(a)] and the decay of the SE curve, indium desorption is taking place. Previous work with Ga on GaN indicates that there is desorption from the droplets and the underlying wetting layer,[11] and it appears that the same is occurring here. During this time, the indium droplets are acting as a reservoir to the wetting layer, resupplying atoms to the desorption-created empty sites of the wetting layer and thereby maintaining it. This continues until the droplets are depleted; subsequently, desorbing adatoms begin reducing the surface coverage of the two-dimensional adlayer, as the SE records in Fig. 2(a). For the fast real-time measurements used here, the gain of each photomultiplier tube in the photodiode array was fixed. Although the detected SE intensity is irrelevant to the extraction of the pseudodielectric function, it can be used as an indicator for the degree of surface scattering. Specifically, if the steady-state coverage is below 2 ML, the intensity stabilizes as the coverage reaches dynamic equilibrium. However, when the $\langle\varepsilon_2\rangle$ value exceeds 2 ML coverage, the intensity decreases without stabilizing but recovers to the original value after the desorption time delay is over and wetting layer desorption starts. This droplet-induced light scattering intensity variation supports the assertion that 2 ML coverage is the threshold for In droplet formation on GaN.

Summarizing, the adsorption-desorption kinetics shown in Fig. 2 occur in five distinct stages: formation of the first monolayer, formation of the second monolayer, droplet formation, desorption of the second monolayer, and, finally, desorption of the first monolayer. Sudden changes in the adsorption-desorption rates before and after the transition point between the first and second monolayers imply that the adsorption-desorption process follows a Kisliuk isotherm: adatoms weakly bound on the covered or uncovered surface migrate until they find the most favorable site.[14] By contrast, if migration was not allowed, formation of the second monolayer could proceed on the partially covered first monolayer simultaneously with the formation of the first monolayer itself. In that case, abrupt adsorption-desorption rate changes are not expected, which is in clear contradiction to the observed data. Thus, it may be concluded that migration of adatoms occurs, allowing the sequential development of the first monolayer, the second monolayer, then droplets. Similarly, during the sequential desorption process, droplets supply indium atoms to the wetting layers, while indium atoms in the second monolayer supply atoms to the first monolayer. At each distinct stage, the formation or desorption of adlayers or droplets occurs only after the completion of the previous stage, but the kinetics is correlated between stages.

IV. ADSORPTION AND DESORPTION RATES

During deposition, impinging atoms adsorb on the surface and a portion of the adsorbates desorb due to thermal fluctuation. So, assuming a linear relationship between $\langle\varepsilon_2\rangle$ and coverage Θ in the nondroplet regime, the inferred adsorption rates obtained from the initial slopes of $\langle\varepsilon_2\rangle$ in Fig. 2(a) represent a net increase in the number of adsorbates on the surface. In the graphs of adsorption rate as a function of

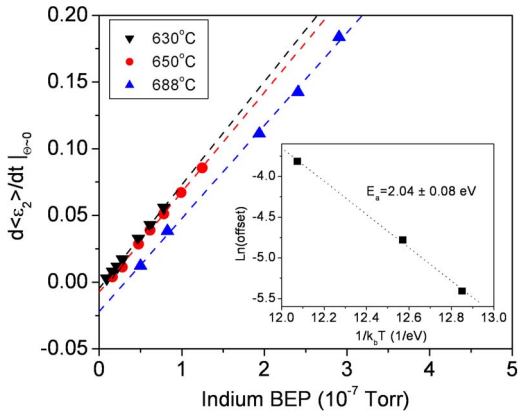

FIG. 3. (Color online) Initial time derivative of the pseudodielectric function from Fig. 2(a), which is measured at the moment the indium shutter is opened ($t=0$, $\Theta\sim 0$), for substrate temperatures of 630, 650, and 688 °C. The observed BEP thresholds correspond to the minimum indium flux required for nuclei formation. The inset is an Arrhenius plot of the extrapolated $k_n^-\Theta_n^{\max}$ for each temperature, which indicates the desorption rate from the nucleation layer.

incident flux (Figs. 3 and 5), the slope indicates the adsorption efficiency. For a given temperature and constant adsorption flux, if the desorption rates r_{des} linearly depend on the adsorbate coverage Θ (i.e., $r_{\text{des}}=k^-\Theta$, where k^- is the rate constant for desorption), then the desorption rate is zero at the moment the deposition starts, and the net adsorption rate linearly increases with the incoming flux. Indeed, the net adsorption rate does depend linearly on the incoming flux, as can be seen in Fig. 3, but the rate extrapolates to zero at a nonzero flux. This lowest required "threshold" flux for deposition to commence increases with increasing temperature, a consequence of the fact that desorption accelerates with increasing temperature. More significantly, this behavior confirms that the first monolayer forms through indium nucleation on the bare GaN surface, just as nuclei were seen to catalyze the formation of the second indium monolayer on the surface of the first indium monolayer.

Thus, for indium flux lower than this threshold BEP at a given temperature, adatom nucleation is thwarted by faster desorption. This indicates that the kinetics of adatom nucleation is different from the deposition kinetics after nuclei formation. The coverage corresponding to this transition ($\Theta_n^{\max}$) is much less than a single monolayer because no delay is observed in the adsorption curve when deposition starts [Fig. 2(a)]. Therefore, the observed thresholds in Fig. 3, which increase with increasing temperature, indicate that nuclei formation precedes layer formation regardless of the high desorption rate constant (k_n^-). The change of adatom kinetics after nucleation implies that the nuclei catalyze subsequent layer formation.

A. First indium monolayer

To quantify these effects, three processes must therefore be considered: adsorption, desorption of nuclei, and desorption from forming layers. The corresponding rate equation is simply

$$\frac{d\Theta}{dt} = k^+ - k_n^-\Theta_n - k_l^-\Theta_l. \tag{1}$$

Here, the subscripts n and l indicate the nucleation and layer formation, respectively, and the total coverage $\Theta=\Theta_n+\Theta_l$ is the sum of the coverage for nucleation (Θ_n) and for the partial layer (Θ_l). In the equation, the first term represents adsorption, which is assumed to be constant since coverage-dependent adsorption processes, such as those characterized by a Langmuir isotherm, only dominate when adatoms do not migrate. The second and third terms are for nucleation desorption and layer desorption, respectively.

In our model, nucleation continues until it reaches a critical coverage, $\Theta_n^{\max}$, after which layer formation ensues as laterally spreading "islands" whose growth is catalyzed around the nuclei. Therefore, the equation for coverage lower than $\Theta_n^{\max}$ is governed by single kinetics with nucleation desorption rate constant k_n^- and total coverage $\Theta=\Theta_n$, so

$$\frac{d\Theta}{dt} = k^+ - k_n^-\Theta \quad (0<\Theta<\Theta_n^{\max}). \tag{2}$$

Referring to Fig. 3, the (temperature-dependent) threshold flux for layer formation to begin corresponds to the flux for which the transition from nucleation to layer formation occurs. Thus, at the initial stage of layer formation, just after sufficient nuclei have adsorbed, the rate equation can be represented as

$$\left.\frac{d\Theta}{dt}\right|_{\Theta=\Theta_n^{\max}} = k^+ - k_n^-\Theta_n^{\max}. \tag{3}$$

The adsorption term k^+ varies linearly with incident flux and the desorption term $k_n^-\Theta_n^{\max}$ therefore equals the minimum adsorption rate required for the transition from nucleation to layer formation, which is manifested as the temperature-dependent threshold BEPs in Fig. 3.

For fluxes higher than this threshold BEP, the impinging adatoms complete the construction of the monolayer through laterally growing nuclei-catalyzed "islands." Desorption occurs from the forming layers ($-k_l^-\Theta_l$) whose desorption rate constant k_l^- is clearly lower than the desorption rate for the nuclei k_n^-. Nuclei adsorption and desorption also occur above $\Theta_n^{\max}$, with additional nuclei created as some adatoms desorb from the growing islands to form new nuclei. Nevertheless, as nuclei catalyze island formation, the total number of nuclei decreases with increasing layer coverage at a rate that is assumed to decrease linearly with increasing layer coverage, i.e., $\Theta_n=\Theta_n^{\max}(1-\Theta_l)$. Thus, for $\Theta_n^{\max}<\Theta<1$, Eq. (1) becomes

$$\frac{d\Theta}{dt} = k^+ - k_n^-\Theta_n^{\max}(1-\Theta_l) - k_l^-\Theta_l$$
$$= \left[k^+ - \frac{k_n^- - k_l^-}{1-\Theta_n^{\max}}\Theta_n^{\max}\right] - \left[\frac{-k_n^-\Theta_n^{\max} + k_l^-}{1-\Theta_n^{\max}}\right]\Theta \quad (4)$$

$$(\Theta_n^{\max} < \Theta < 1 \text{ ML}),$$

and the measured growth rate represents the net result of these competing processes of adsorption and desorption. Referring to Fig. 3 and extrapolating the data for a given temperature to $k^+=0$ incident flux (i.e., the y intercept) yields the value for $k_n^-\Theta_n^{\max}$, which also corresponds to the threshold value (i.e., the x intercept) for the 1 ML case. An Arrhenius plot of $k_n^-\Theta_n^{\max}$ as a function of temperature (inset of Fig. 3) indicates that the activation energy for nuclei desorption from the GaN (0001) surface is 2.04 ± 0.08 eV.

The activation energy for layer desorption may be obtained by a similar analysis of the decaying signal following indium off in Fig. 2(a). Concentrating for the moment only on the decay below 1 ML, it is readily apparent that the decay is independent of the preceding incident flux, except possibly for the highest fluxes which lead to droplet formation. Desorption occurs through two processes: desorption from the monolayer into the vacuum above and desorption from the monolayer into nuclei. If desorption for $\Theta \leq 1$ ML only occurred by releasing adsorbed atoms into the vacuum, the governing equation would simply be Eq. (1) with $k^+ = k_n^- = 0$, namely,

$$\frac{d\Theta}{dt} \approx -k_l^-\Theta, \quad (5a)$$

leading to a simple exponential decay. Instead, analysis of the decay curve in Fig. 2(a) indicates decay in the form of (single exponential+constant). This is the form of the solution of rate equation [Eq. (4)] with $k^+=0$,

$$\frac{d\Theta}{dt} = -\frac{k_n^- - k_l^-}{1-\Theta_n^{\max}}\Theta_n^{\max} - \left[\frac{-k_n^-\Theta_n^{\max} + k_l^-}{1-\Theta_n^{\max}}\right]\Theta, \quad (5b)$$

strongly suggesting that desorption from the layer to nuclei is also taking place and even becomes the predominant mechanism as the coverage shrinks. Nevertheless, k_l^- may be easily obtained by fitting the slope of the measured decay at $\Theta \approx 1$ ML since there can be no desorption to nuclei with full monolayer coverage.

Figure 4 measures the expected acceleration of desorption with temperature for the $0<\Theta<1$ ML region. From the fitted slopes (straight lines in Fig. 4), the activation energy for desorption from the completed first monolayer, calculated from the Arrhenius plot of the k_l^- in the inset, is 2.64 ± 0.2 eV. This value is only slightly higher than the sublimation energy of bulk indium (2.52 eV),[15] suggesting that desorption from the first monolayer on bare GaN (0001) primarily involves breaking In(adatom)-In(adatom) bonds, while the weak influence of In(adatom)-Ga(surface) bonds may account for the difference of these energies.

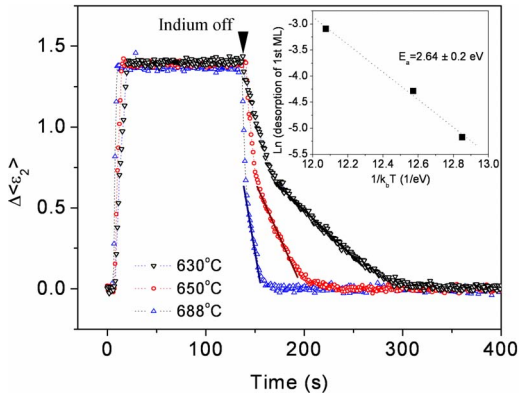

FIG. 4. (Color online) Desorption curves after 2 ML deposition under substrate temperatures of 630, 650, and 688 °C. The temperature-dependent desorption rates measured after $\Delta\langle\varepsilon_2\rangle$ falls to ~0.7 (i.e., 1 ML coverage) reveal the activation energy for desorption from the first monolayer to be 2.64 eV (inset).

B. Second indium monolayer

The kinetic processes responsible for the growth of and desorption from the second monolayer are identical to the first monolayer. Equations similar to Eqs. (1)–(4), (5a), and (5b) may therefore be used to describe the growth thresholds and desorption activation energies of the second monolayer also. Indeed, like the first monolayer, the second monolayer also has a temperature-dependent adsorption "second threshold," followed by lateral growth of the second monolayer that accelerates with increasing flux. However, an additional process must be considered, namely, that of the loss of adatoms from the second monolayer to replenish those vacancies created by desorption from the portion of the first monolayer that remains exposed. This process grows less important as the coverage of the second monolayer increases, namely,

$$\frac{d\Theta_2}{dt} = k^+ - k_{n2}^-\Theta_{n2} - k_{l2}^-\Theta_{l2} - k_l^-(1-\Theta_2), \quad (6)$$

where Θ_2 represents the coverage of the second monolayer ($\Theta_2=\Theta_{n2}+\Theta_{l2}$) and the rate constants for the second monolayer are indicated by the additional subscript "2."

Figure 5 plots $d\langle\varepsilon_2\rangle/dt$, which is measured at the moment when $\Theta=1$ ML ($\langle\varepsilon_2\rangle=0.9$), as a function of incident flux for each temperature. In this figure, two regimes are observed in the data for a given temperature. First, the slope is zero as the flux increases, representing second monolayer nucleation on the completed first monolayer. Then, the slope linearly increases from a temperature-dependent threshold flux, representing layer formation around the second monolayer nuclei.

Of the zero slope data points, the lowest flux value at a given temperature corresponds to the minimum flux required to maintain steady-state coverage of 1 ML. Similarly, the second threshold, where the transition from zero to nonzero slope occurs, is the minimum flux required to maintain the first monolayer as well as the nucleation layer for the second monolayer. In other words, the second threshold arises from the adatom flux sufficient to enable transfer of indium ada-

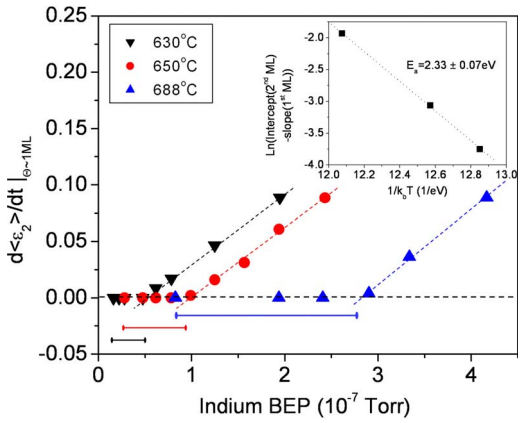

FIG. 5. (Color online) Time derivative of the pseudodielectric function from Fig. 2(a) measured at the moment when $\Theta \sim 1$ ML for substrate temperatures of 630, 650, and 688 °C. The observed BEP second thresholds correspond to the minimum indium flux required to maintain the first monolayer and nucleation of the second monolayer. By compensating the minimum indium flux needed to maintain the first monolayer from the desorption curve in Fig. 4, the activation energy for nucleation of the second monolayer is found to be 2.33 eV (inset).

toms to sites of the first monolayer emptied by desorption as well as enough nuclei for the second monolayer to begin forming. Simplifying Eq. (6) for the case of threshold in much the same way as was done for Eq. (3), we obtain

$$\left.\frac{d\Theta_2}{dt}\right|_{\Theta_2=\Theta_{n2}^{\max}} = k^+ - k_{n2}^- \Theta_{n2}^{\max} - k_l^-(1-\Theta_{n2}^{\max}). \quad (7)$$

Thus, after compensating for desorption from the exposed desorbing first monolayer by adding the corresponding first monolayer desorption rate k_l^- to this second y intercept $(k_{n2}^- \Theta_{n2}^{\max} - k_l)$, the actual desorption rate from the second monolayer nuclei can be extracted. The resulting activation energy for nucleation in the second monolayer is 2.33 ± 0.07 eV (inset of Fig. 5), which is higher than the activation energy for nuclei desorption from the first monolayer.

Similarly, desorption from the completed second monolayer proceeds in much the same manner as desorption from the completed first monolayer, through a combination of desorption into the vacuum and desorption forming nuclei. In addition, a third process occurs, namely, desorption to fill voids in the underlying first monolayer caused by desorption from that increasingly exposed layer. This additional process is clearly very active, explaining the steeper decay slope for 1 ML $< \Theta <$ 2 ML than for 0 ML $< \Theta <$ 1 ML, as well as the "kink" in the decay curve at $\Theta = 1$ ML when this additional process ceases. The rate equation for second monolayer desorption is similar to Eq. (5b), which at $\Theta = 2$ ML simplifies to an equation much like Eq. (5a),

$$\frac{d\Theta_2}{dt} \approx -k_{l2}^- \Theta_2. \quad (8)$$

Thus, by measuring the slope of the decay at $\Theta = 2$ ML, the desorption rate k_{l2}^- may be obtained. The corresponding activation energy for desorption from the completed second monolayer was found to be 2.53 ± 0.18 eV, which is virtually equal to the sublimation energy and slightly lower than the corresponding first monolayer value. The difference between the 1 and 2 ML activation energies (2.53 eV vs 2.64 eV) appears physically meaningful and may be due to the additional effect of In-Ga bonding in the first monolayer. The extracted activation energies for desorption from both 1 and 2 ML are comparable to the result of 2.7 eV reported by Monroy *et al.*[4]

TABLE I. Desorption activation energies for In on a GaN [0001] surface.

	First monolayer (eV)	Second monolayer (eV)
Nucleation	2.04 ± 0.08	2.33 ± 0.07
Full layer	2.64 ± 0.20	2.53 ± 0.18

V. SUMMARY

In summary, we measured the indium adsorption-desorption kinetics on the GaN (0001) surface using *in situ* spectroscopic ellipsometry. At the beginning of each monolayer formation, precursor nuclei bond with the dangling bonds, terminating the underlying surfaces. After the nuclei formation, they mediate the adsorption of subsequent indium adatoms *through the preferential* formation of In-In (adatom-nuclei) bonds, which are more stable than In-Ga bonds (adatom-surface). Thus, after the formation of the nuclei, subsequent incoming atoms adsorb primarily by bonding with these nuclei, causing lateral island growth. The rapid increase in the steady-state coverage after nuclei formation, as a function of incident flux, further supports the conclusion of separate nucleation and lateral growth mechanisms.

A single model is proposed to explain (1) the existence of two stable monolayers, (2) thresholds for the onset of layer growth for the first two monolayers, and (3) bicomponent desorption curves. The derived nucleation and complete layer desorption activation energies of indium adatoms are summarized in the Table I. The activation energies for the nuclei for each monolayer are lower than the activation energies for fully covered layers, which is consistent with the fact that the surface-adatom interaction is weaker than the adatom-adatom interaction. This observation explains the segregation characteristics of indium atoms widely observed in III-N semiconductor growth. The lower activation energy of nuclei in the first monolayer implies that only nuclei formation on bare GaN involves interaction with the surface, while all subsequent kinetics involves In-In interactions.

ACKNOWLEDGMENTS

We gratefully acknowledge J. Northrup for valuable discussions. This work was supported by the ONR/DARPA through Contract No. 00014-3-1-0608.

[1] J. E. Northrup and J. Neugebauer, Phys. Rev. B **60**, R8473 (1999).
[2] J. Neugebauer, T. K. Zywietz, M. Scheffler, J. E. Northrup, H. Chen, and R. M. Feenstra, Phys. Rev. Lett. **90**, 056101 (2003).
[3] F. Jiang, R.-V. Wang, A. Munkholm, S. K. Streiffer, G. B. Stephenson, P. H. Fuoss, K. Latifi, and Carol Thompson, Appl. Phys. Lett. **89**, 161915 (2006).
[4] E. Monroy, B. Daudin, E. Bellet-Amalric, N. Gongneau, D. Jalabert, F. Enjalbert, J. Brault, J. Barjon, and L. S. Dang, J. Appl. Phys. **93**, 1550 (2003).
[5] F. Widmann, B. Daudin, G. Feuillet, N. Pelekanos, and J. L. Rouvière, Appl. Phys. Lett. **73**, 2642 (1998).
[6] H. Yuan, S. J. Chua, S. Tripathy, and P. Chen, J. Vac. Sci. Technol. A **21**, 1814 (2003).
[7] O. Mayrock, H.-J. Wünsche, and F. Henneberger, Phys. Rev. B **62**, 16870 (2000).
[8] P. Waltereit, O. Brandt, K. H. Ploog, M. A. Tagliente, and L. Tapfer, Phys. Status Solidi B **228**, 49 (2001).
[9] J. R. Jinschek, R. Erni, N. F. Gardner, A. Y. Kim, and C. Kisielowski, Solid State Commun. **137**, 230 (2006).
[10] H. G. Tompkins, *A User's Guide to Ellipsometry* (Academic Press, Boston, 1993), pp. 65–81.
[11] S. Choi, T. Kim, A. Brown, H. Everitt, M. Losurdo, G. Bruno, and A. Moto, Appl. Phys. Lett. **89**, 181915 (2006).
[12] R. M. Feenstra, J. E. Northrup, and J. Neugebauer, MRS Internet J. Nitride Semicond. Res. **7**, 3 (2002).
[13] H. Fujiwara, *Spectroscopic Ellipsometry: Principles and Applications* (Wiley, New York, 2007), pp. 184–187.
[14] P. Kisliuk, J. Phys. Chem. Solids **3**, 95 (1957).
[15] C. Kittel, *Einführung in die Festkörperphysik* (R. Oldenbourg, Munich, 1999).